TÜBİTAK

Turkish Journal of Chemistry

http://journals.tubitak.gov.tr/chem/

Research Article

Turk J Chem
(2015) 39: 660 – 666

doi:10.3906/kim-1410-58

Characterization of a Cu^{2+}-selective fluorescent probe derived from rhodamine B with 1,2,4-triazole as subunit and its application in cell imaging

Na LI, Chunwei YU, Yuxiang JI, Jun ZHANG*
Department of Environmental Sciences, School of Tropical and Laboratory Medicine, Hainan Medical College, Haikou, P.R. China

Received: 25.10.2014 • **Accepted/Published Online:** 09.03.2015 • **Printed:** 30.06.2015

Abstract: A rhodamine B derivative containing 1,2,4-triazole as subunit was characterized as an "off–on" type Cu^{2+}-selective fluorescent probe. It exhibited high selectivity and sensitivity for Cu^{2+} in ethanol–water solution (9:1, v:v, pH 7.0, 20 mM HEPES) and underwent ring opening. A prominent fluorescence enhancement at 570 nm was observed in the presence of Cu^{2+} with the change in the absorption spectrum, and a 1:1 metal–ligand complex was formed. With the optimized experimental conditions, the probe exhibited a dynamic response range for Cu^{2+} from 8.0×10^{-7} to 7.5×10^{-6} M with a detection limit of 2.3×10^{-7} M in ethanol–water solution (9:1, v:v, pH 7.0, 20 mM HEPES). Its application in Cu^{2+} imaging in living cells was also studied.

Key words: Fluorescent probe, rhodamine B, triazole, Cu^{2+}

1. Introduction

The detection of heavy transition-metal ions has attracted a lot of interest recently.[1–3] Among them, copper is an essential trace element in both plants and animals, including humans. Deficiency and excess of copper could cause serious imbalance of human body functions, which damage the human brain and multiple systems.[4–7] Therefore, the development of methods for easy detection of Cu^{2+} is of great importance for the environment and human health. Compared with the conventional methods for detecting Cu^{2+}, such as atomic absorption spectrometry (AAS), inductively coupled plasma-atomic emission spectrometry (ICP-AES), and inductively coupled plasma-mass spectroscopy (ICP-MS), fluorescence spectroscopy displayed high selectivity and sensitivity, was easy to operate, and had low detection limits. In addition, the equipment of detection was simple without complex multistage sample preparation.[8–12]

The property of the probes was determined by the fluorophore and recognition site. It is well known that rhodamine B was always chosen as fluorophore because of its unique structural characteristics and photophysical properties, that is, it appeared colorless and nonfluorescent in spirolactam form, but displayed remarkable color change and fluorescence in the ring-opened amide.[13–17] The selectivity and sensitivity of a probe was mainly decided by the recognition sites. 1,2,4-Triazole has lone electron pairs on N, which provide good coordination property to metal ions, and several 1,2,4-triazole containing host compounds have been synthesized for the detection of Cu^{2+}.[13] According to the soft–hard acid–base theory, S shows good affinity to Cu^{2+}, and so a –SH group was introduced in the system to improve the coordination ability of probe **P**. Furthermore, the

*Correspondence: jun_zh1979@163.com

semirigid property of 1,2,4-triazole containing complex could effectively chelate Cu^{2+} according to the ionic radius and also limit the geometric structure of the complex. In the present work, a Cu^{2+}-selective fluorescent probe derived from rhodamine B containing 1,2,4-triazole as subunit was proposed (Figure 1). Its application for imaging Cu^{2+} in living cells was also described.

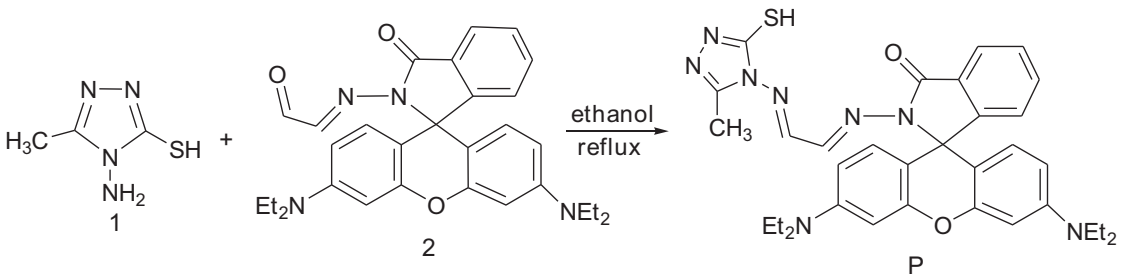

Figure 1. Synthesis route of probe **P**.

2. Results and discussion

2.1. Effect of pH on P and P with Cu^{2+}

The pH dependence of the fluorescence intensity of **P** and the **P**–Cu^{2+} system is shown in Figure 2. The results revealed that the fluorescence of the free **P** could be negligible; however, a significant fluorescence enhancement was observed upon the addition of Cu^{2+}, which was attributed to the opening of the spirolactam ring of the rhodamine unit. These data demonstrated that **P** could work within a wide pH range of 5.8–8.4, which made it possible for the detection of Cu^{2+} under physiological pH conditions. To exclude the influence of acidity on the test, pH 7.0 was fixed in the further research.

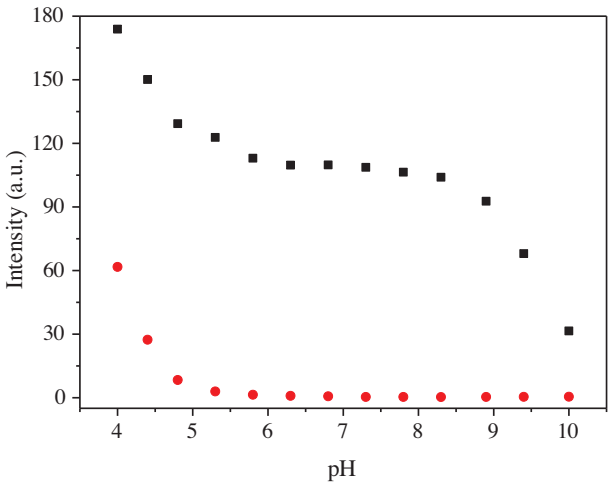

Figure 2. pH-dependent fluorescence of **P** (10 μM) (●, in red) and **P** (10 μM) plus 100 μM Cu^{2+} (■) in HEPES buffers as a function of different pH values.

2.2. Uv-vis spectral response of P

In the UV-vis spectrum of **P**, the absorption with various metal ions was recorded in ethanol–water solution (9:1, v:v, pH 7.0, 20 mM HEPES) (Figure 3). The results showed that a peak at 556 nm appeared with the addition of Cu^{2+}, and the colorless solution of **P** was changed to an intense pink due to the spirolactam ring

opening of the rhodamine unit. Hg^{2+} and Ni^{2+} had negligible interference, while other metal ions, such as Na^{+}, K^{+}, Ag^{+}, Ca^{2+}, Mg^{2+}, Zn^{2+}, Pb^{2+}, Cd^{2+}, Co^{2+}, Mn^{2+}, and Cr^{3+} did not show any influence on the absorbance of **P** under identical conditions.

2.3. Fluorescence spectral response of P

The fluorescence property of **P** was measured to investigate the probe's selectivity in ethanol–water solution (9:1, v:v, pH 7.0, 20 mM HEPES) with addition of different metal ions (Figure 4). Compared with other tested metal ions, only Cu^{2+} caused a significant "turn-on" fluorescence response at 575 nm, and Hg^{2+} had negligible interference. It indicated that **P** could selectively recognize Cu^{2+} in ethanol–water solution (9:1, v:v, pH 7.0, 20 mM HEPES) and the interference of other tested metal ions in the detection of Cu^{2+} could be negligible.

In the emission spectra (Figure 5), the fluorescence peak at 575 nm increased upon the addition of Cu^{2+}; the linear portion of the plot of fluorescence intensity vs. Cu^{2+} could be used to detect the unknown concentration of Cu^{2+} over the range of 8.0×10^{-7} to 7.5×10^{-6} M with a detection limit of 2.3×10^{-7} M.

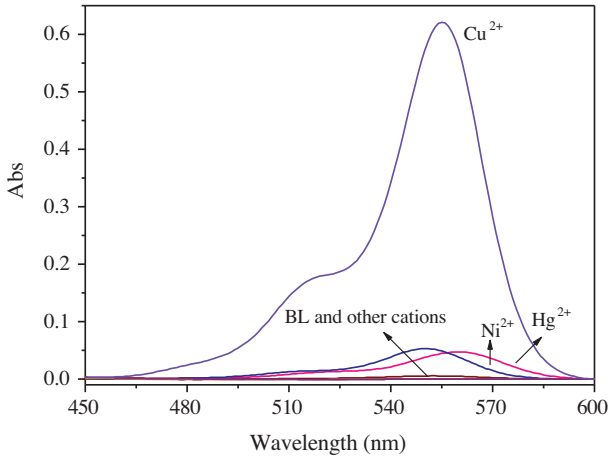

Figure 3. UV-vis spectra of **P** (10 μM) with different metal ions (100 μM) in ethanol–water solution (9:1, v:v, pH 7.0, 20 mM HEPES).

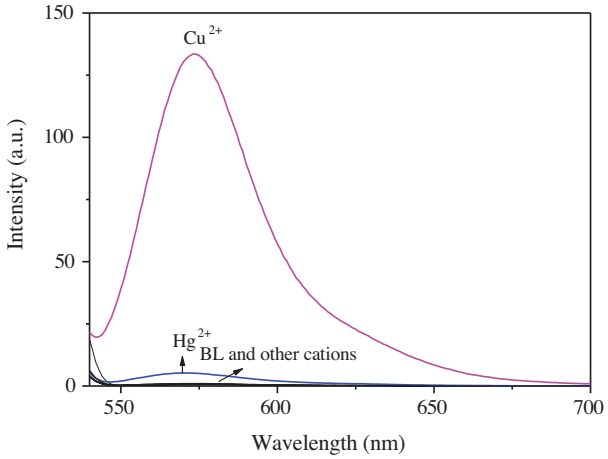

Figure 4. Fluorescence spectra of **P** (10 μM) with different metal ions (100 μM) in ethanol–water solution (9:1, v:v, pH 7.0, 20 mM HEPES).

One challenge for the probe is to obtain a specific detection system for Cu^{2+} over a wide range of potentially competing ions, since the system might show cross-sensitivity toward other metal ions. Therefore, the competition experiments were conducted in the presence of 1 equiv. of Cu^{2+} mixed with 5 equiv. of other metal ions as mentioned above. No significant variation in fluorescence intensity was found by comparison with the same amounts of Cu^{2+} solution without other metal ions, and the relative error was less than $\pm 5\%$ (Figure 6). For probe **P**, cross-sensitivity to the other metal ions was not observed, while an excellent selectivity toward Cu^{2+} was exhibited. Thus, it indicated that the probe **P** was a Cu^{2+}-specific fluorescent probe.

2.4. The proposed reaction mechanism

The Job's plot was drawn to prove the complex ratio of **P** with Cu^{2+} (Figure 7). Total concentration of **P** and Cu^{2+} was kept at a fixed 50 μM. The results showed that the maximum fluorescent emission intensity of **P**–Cu^{2+} complex appeared at 0.5, which indicated that a **P**–Cu^{2+} complex was formed in 1:1 mole ratio.

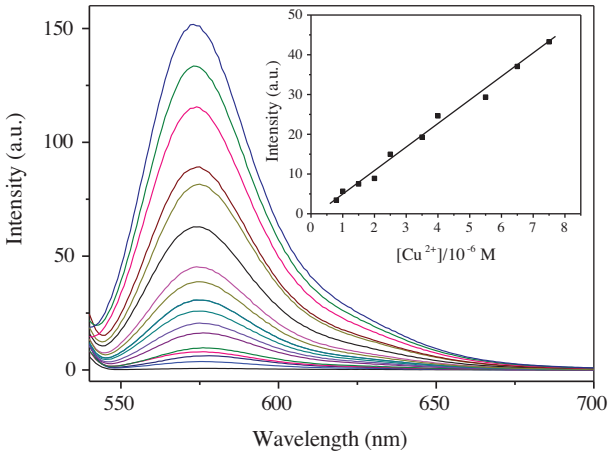

Figure 5. Fluorescence response of **P** (10 μM) with various concentrations of Cu^{2+} in ethanol–water solution (9:1, v:v, pH 7.0, 20 mM HEPES).

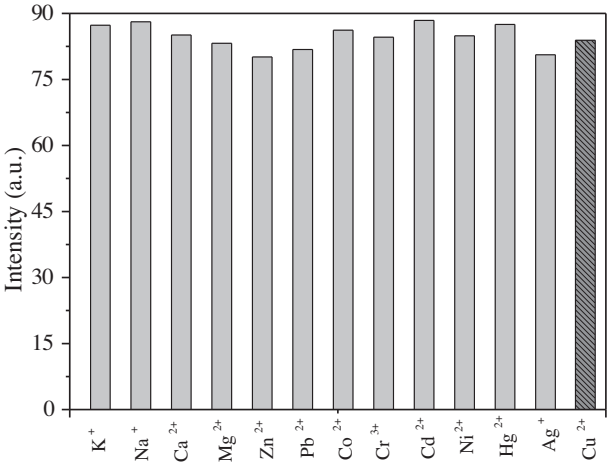

Figure 6. Fluorescence response of **P** (10 μM) to Cu^{2+} ions (10 μM) or to a mixture of the specified metal ions (50 μM) with Cu^{2+} ions (10 μM) in ethanol–water solution (9:1, v:v, pH 7.0, 20 mM HEPES).

To further understand the reaction mechanism of probe **P** to Cu^{2+}, EDTA titration experiments were conducted to examine the reversibility of the probe **P** with Cu^{2+} (Figure 8). Upon the addition of 50 μM EDTA to the mixture of **P** (10 μM) and Cu^{2+} (10 μM) in ethanol–water solution (9:1, v:v, pH 7.0, 20 mM HEPES), the fluorescent emission intensity of **P**–Cu^{2+} was significantly reduced and the color changed from pink to almost colorless. When Cu^{2+} was added to the system again, the signals were almost completely reproduced, and the colorless solution turned pink. The results demonstrated that the binding of **P** and Cu^{2+}

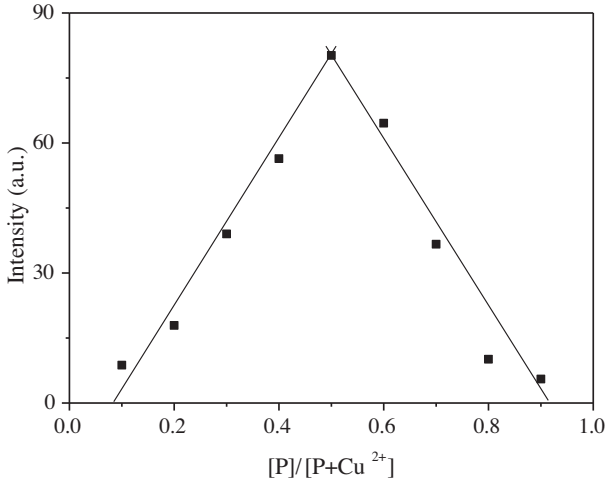

Figure 7. Job's plot of **P** with Cu^{2+} according to the method of continuous variation. The total concentration of **P** and Cu^{2+} was 50 μM.

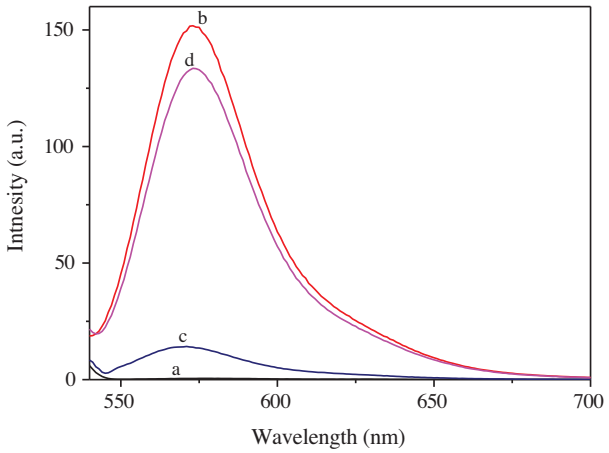

Figure 8. Reversible titration response of **P** to Cu^{2+} in ethanolwater solution (9:1, v:v, pH 7.0, 20 mM HEPES): (a) **P** (10 μM); (b) **P** (10 μM) + Cu^{2+} (10 μM); (c) **P** (10 μM) + Cu^{2+} (10 μM) + EDTA (50 μM); (d) **P** (10 μM) + Cu^{2+} (10 μM) + EDTA (50 μM) + Cu^{2+} (0.1 mM).

was a reversible process. According to the experimental results, the reaction mechanism was proposed as shown in Figure 9.

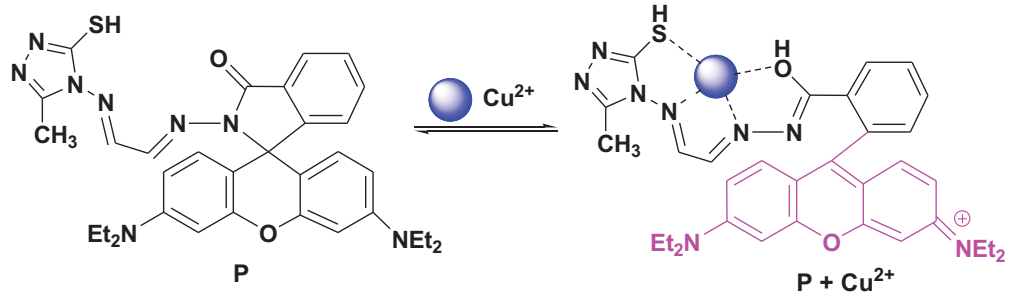

Figure 9. Proposed binding mode of **P** and Cu^{2+}.

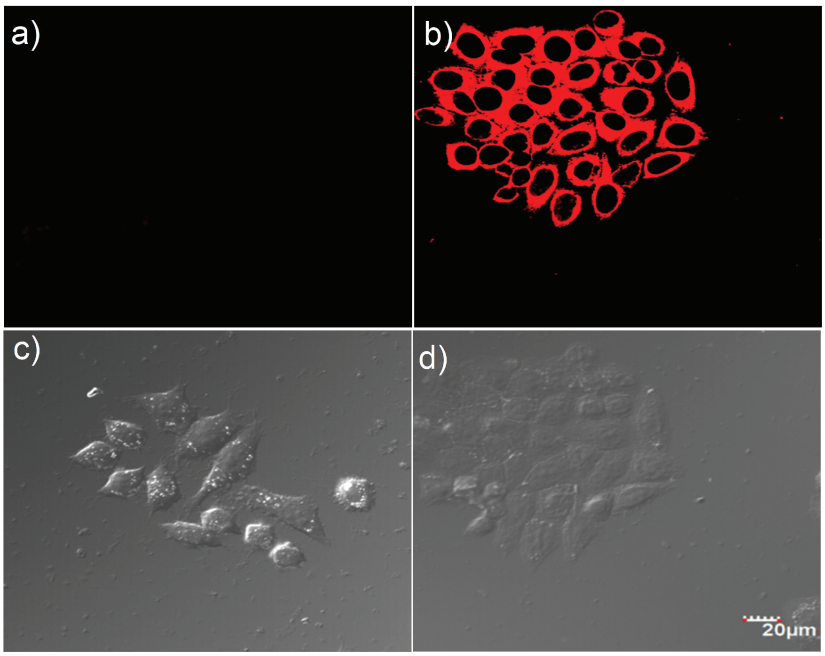

Figure 10. Confocal fluorescence and brightfield images of HepG2 cells. a) Cells stained with 10 μM P for 30 min at 37 °C; b) cells supplemented with 1 μM $CuCl_2$ in the growth media for 30 min at 37 °C and then incubated with 10 μM P for 30 min at 37 °C; c) bright field image of cells shown in a); d) bright field image of cells shown in b).

2.5. Preliminary analytical application

To further demonstrate the practical applicability of the probe **P**, confocal microscopy experiments were further carried out, and the fluorescence images of HepG2 cells were recorded before and after the addition of Cu^{2+} (Figure 10). The cells incubated with **P** for 30 min at 37 °C showed very weak fluorescence, as shown in Figure 10a. When cells stained with **P** were incubated with $CuCl_2$ (1 μM), the color of the HepG2 cells showed significant changes (Figure 10b). The bright field images of Figure 10a and Figure 10b were shown as Figure 10c and Figure 10d, and the shapes of cells indicated that **P** has low toxicity. These results suggested that probe **P** can penetrate the cell membrane and might be used for detecting Cu^{2+} in living cells.

In conclusion, a novel Cu^{2+}-selective rhodamine B fluorescent probe containing 1,2,4-triazole as subunit was constructed. Cu^{2+} could induce spirolactam ring opening of the rhodamine unit and achieved an "off–on" effect. The probe **P** can detect as low as 2.3×10^{-7} M Cu^{2+}. In addition, the probe **P** was successfully used to detect Cu^{2+} in living cells.

3. Experimental

3.1. Reagents and instruments

All reagents and solvents are of analytical grade and used without further purification. The metal ions and anions salts employed were NaCl, KCl, $CaCl_2 \cdot 2H_2O$, $MgCl_2 \cdot 6H_2O$, $Zn(NO_3)_2 \cdot 6H_2O$, $PbCl_2$, $CdCl_2$, $CrCl_3 \cdot 6H_2O$, $CoCl_2 \cdot 6H_2O$, $NiCl_2 \cdot 6H_2O$, $HgCl_2$, $CuCl_2 \cdot 2H_2O$, $FeCl_3 \cdot 6H_2O$, and $AgNO_3$.

Fluorescence emission spectra were conducted on a Hitachi 4600 spectrofluorometer. UV-Vis spectra were obtained on a Hitachi U-2910 spectrophotometer. Nuclear magnetic resonance (NMR) spectra were measured with a Bruker AV 400 instrument and chemical shifts are given in ppm from tetramethylsilane (TMS). Mass spectra (MS) were recorded on a Thermo TSQ Quantum Access Agilent 1100.

3.2. Synthesis of compound P

Compounds **1** and **2** were synthesized as reported.[18,19]

Compounds **1** (0.13 g, 1.0 mM) and **2** (0.496 g, 1.0 mM) were mixed in ethanol (40 mL). The reaction mixture was stirred at 80 °C for 4 h. After the reaction was finished, the solution was removed under reduced pressure. The precipitate so obtained was filtered and purified with silica gel column chromatography (petroleum ether/acetic ether = 5:1, v:v) to afford **P** as yellow solid. Yields: 83.4%. MS (ES+) m/z: 609.27 $[M + H]^+$. ^{1}H NMR (δ ppm, d_6-DMSO): ^{1}H NMR: 13.74 (s, 1H), 9.82 (d, 1H, $J = 8.2$), 8.34 (d, 1H, $J = 8.2$), 7.96 (d, 1H, $J = 7.4$), 7.65 (t, 1H, $J = 7.4$), 7.58 (t, 1H, $J = 7.4$), 6.45 (t, 4H, $J = 8.3$), 6.63 (t, 2H, $J = 10.8$), 7.08 (d, 1H, $J = 7.6$), 3.32 (m, 8H, $J = 8.4$), 2.21 (s, 3H), 1.08 (t, 12H, $J = 7.8$). ^{13}C NMR (δ ppm, d_6-DMSO): 165.57, 161.88, 159.59, 153.19, 152.85, 149.62, 149.52, 143.24, 135.85, 132.41, 129.93, 129.55, 128.50, 127.88, 124.83, 124.42, 109.23, 105.17, 98.32, 66.49, 65.92, 44.57, 30.91, 19.55, 14.44, 13.29, 11.52, 11.29.

3.3. General spectroscopic methods

Metal ions and chemosensor **P** were dissolved in deionized water and DMSO to obtain 1.0 mM stock solutions, respectively. Before spectroscopic measurements, the solution was freshly prepared by diluting the high concentration stock solution with the corresponding solution. For all measurements, excitation/emission slit widths were 5/10 nm and excitation wavelength was 550 nm.

Acknowledgments

This work was financially supported by the National Natural Science Foundation of China (No. 81260268, 81360266), the Natural Science Foundation of Hainan Province (No. 812188, 413131), and the Colleges and Universities Scientific Research Projects of the Education Department of Hainan Province (Hjkj2013-29).

References

1. Nolan, E. M.; Lippard, S. J. *Chem. Rev.* **2008**, *108*, 3443–3480.
2. Jeong, Y.; Yoon, J. *Inorg. Chim. Acta* **2012**, *381*, 2–14.

3. Xu, Z. C.; Yoon, J.; Spring, D. R. *Chem. Soc. Rev.* **2010**, *39*, 1996–2006.
4. Radisky, D.; Kaplan, J. *J. Biol. Chem.* **1999**, *274*, 4481–4484.
5. Rode, B. M.; Suwannachot, Y. *Coordin. Chem. Rev.* **1999**, *190–192*, 1085–1099.
6. Tapiero, H.; Townsend, D. M.; Tew, K. D. *Biomed. Pharmacother.* **2003**, *57*, 386–398.
7. Kwon, H.; Lee, K.; Kim, H. J. *Chem. Comm.* **2011**, *47*, 1773–1775.
8. Peng, X. J.; Du, J. J.; Fan, J. L.; Wang, J. Y.; Wu, Y. K.; Zhao, J. Z.; Sun, S. G.; Xu, T. *J. Am. Chem. Soc.* **2007**, *129*, 1500–1501.
9. Huang, J. H.; Xu, Y. F.; Qian, X. H. *Dalton Trans.* **2009**, *10*, 1761–1766.
10. Lee, M. H.; Kim, H. J.; Yoon, S. W.; Park, N. J.; Kim, J. S. *Org. Lett.* **2008**, *10*, 213–216.
11. Wu, D. Y.; Huang, W.; Duan, C. Y.; Lin, Z. H.; Meng, Q. J. *Inorg. Chem.* **2007**, *46*, 1538–1540.
12. Yang, X. F.; Guo, X. Q.; Zhao, Y. B. *Talanta* **2002**, *57*, 883–890.
13. Zhang, J.; Yu, C. W.; Qian, S. Y.; Lu, G.; Chen, J. L. *Dyes Pigm.* **2012**, *92*, 1370–1375.
14. Du, J. J.; Fan, J. L.; Peng, X. J.; Sun, P. P. *Org. Lett.* **2010**, *12*, 476–479.
15. Weerasinghe, A. J.; Abebe, F. A.; Sinn, E. *Tetrahedron Lett.* **2011**, *52*, 5648–5651.
16. Kim, H.; Lee, M.; Kim, H.; Kim, J.; Yoon, J. *Chem. Soc. Rev.* **2008**, *37*, 1465–1472.
17. Yu, C. W.; Zhang, J.; Wang, R.; Chen, L. X. *Org. Biomol. Chem.* **2010**, *8*, 5277–5279.
18. Yu, C. W.; Zhang, J.; Li, J. H.; Liu, P.; Wei, P. H.; Chen, L. X. *Microchim. Acta* **2011**, *174*, 247–255.
19. Liu, C. Y.; Zhao, Q. Q.; Li, J. *Chem. Reagents* **2001**, *23,* 344–345 (in Chinese).